Ecotoxicology
DOI 10.1007/s10646-015-1594-6

Subcellular distribution, modulation of antioxidant and stress-related genes response to arsenic in *Brassica napus* L.

Muhammad A. Farooq[1] · Rafaqat A. Gill[1] · Basharat Ali[1] · Jian Wang[1] · Faisal Islam[1] · Shafaqat Ali[2] · Weijun Zhou[1]

Accepted: 16 November 2015

Abstract Arsenic (As) is an environmental toxin pollutant that affects the numerous physiological processes of plants. In present study, two *Brassica napus* L. cultivars were subjected to various concentrations (0, 50, 100, and 200 μM) of As for 14 days, plants were examined for As subcellular distribution, photosynthesis parameters, oxidative stress, and ultrastructural changes under As-stress. Differential fraction analysis showed that significant amount of As was accumulated in the cell wall as compared to other organelles. Decline in photosynthetic efficiency under As stress was observed in term of reduced pigment contents and gas exchange parameters. Differential responses of antioxidants at both enzymatic and gene levels to higher As stress were more pronounced in cultivar ZS 758 as compared to Zheda 622. The qRT-PCR analysis showed that heat shock protein 90 (*Hsp90*) and metallothionein were over-expressed in As stressed *B. napus* plants. Disorganization of cell structure and the damages in different organelles were some of the obvious variations in cultivar Zheda 622 as compared to ZS 758.

Keywords Arsenic toxicity · Antioxidant enzyme activities · *Brassica napus* L. · Oxidative stress · Subcellular fractions

✉ Weijun Zhou
wjzhou@zju.edu.cn

[1] Institute of Crop Science and Zhejiang Key Laboratory of Crop Germplasm, Zhejiang University, Hangzhou 310058, China

[2] Department of Environmental Sciences and Engineering, Government College University, Faisalabad 38000, Pakistan

Introduction

Arsenic (As) stands at 20th rank according to its abundance on the earth's crust and considers among the few elements which are yet to be characterized as a single element (Shanker 2008). As is widely distributed in trivalent or pentavalent form on the earth crust. Most common occurring trivalent (3^+) inorganic compounds are sodium arsenite, arsenic trioxide and arsenic trichloride, whereas pentavalent (5^+) inorganic compounds are arsenic acid, arsenates and arsenic pent-oxide (Shanker 2008). As (V) is probably reduced to As (III) inside the cell (Zhao et al. 2009). Arsenate competes with the phosphate in metabolic processes and arsenite makes the binding to –SH groups of proteins, thus altering protein structure or interfering the catalytic sites of enzymes (Shen et al. 2013).

Although, As is a non-redox-active metalloid and evidences showed that As exposure induces the generation of reactive oxygen species (ROS) that cause oxidative stress in plants (Leterrier et al. 2012; Sharma 2012), which could result in lipid peroxidation and associated toxicity (Singh et al. 2006). Oxidative stress due to As exposure is the main process underlying the arsenic toxicity in plants (Shri et al. 2009). Naturally plants have detoxification strategies to respond the oxidative stress through the activation of various enzymatic or non-enzymatic antioxidants such as superoxide dismutase (SOD), ascorbate peroxidase (APX), catalase (CAT), guaiacol peroxidase (POD) and glutathione (GR). Different antioxidant enzyme activities (SOD, POD, CAT APX and GR) and their corresponding genes have been studied in many plant species under different stress conditions (Rout and Sahoo 2013; Luo et al. 2011). Transcript levels of SOD, POD, CAT, APX and GR were strongly induced under chromium (Cr), cadmium (Cd) and copper (Cu) toxicity, and the over expression of

Published online: 23 November 2015

these specific antioxidant genes conferred the tolerance to various metal stresses (Gill et al. 2015; Ahammed et al. 2013; Rout and Sahoo 2013).

Arsenic stress tolerance mechanism differs not only among plant species but also for cultivars and genotypes of the same species (Austruy et al. 2013; Rahmana et al. 2007). A wide range of defense mechanisms have been evolved by the plants to tolerate and survive in heavy metal polluted environment. These defensive strategies comprise of restricted distribution of toxic metal in sensitive tissues, chelation by organic molecules and metal compartmentalization into the vacuoles (Caldelas et al. 2012). Localization of heavy metals in plant tissues and their distribution at subcellular is closely linked to their toxicity (Zeng et al. 2011). Heavy metal like lead (Pb) is mainly found both in the cell wall and vacuoles (Wu et al. 2013), and similar pattern of subcellular distribution of metal in cell wall has been reported in rice (*Oryza sativa* L.) (Zeng et al. 2011).

Indian mustard (*Brassica juncea* L.), Alpine Pennygrass (*Noccaea caerulescens* L.) and oilseed rape (*Brassica napus* L.) are Brassicaceae family members. These plants have high ability to tolerate and accumulate heavy metals in their tissues. Oilseed rape (*B. napus*) can be used as a crop for phytoremediation because of its relatively higher biomass, which could extract more heavy metals from the soil compared to other crop species (Grispen et al. 2006). The aim of the work reported here was to determine the toxic effects of As on two *B. napus* cultivars. Firstly, the effect of different As concentrations on plant dry biomass, photosynthesis and oxidative stress as well as their subcellular localization in plant tissues through histochemical analysis were estimated. Secondly, the subcellular distribution of As in different plant organelles were measured. Thirdly, the transcript level of stress responsive gene (*Hsp90* and *MT*) and antioxidants enzymes activity as well as their related genes expression were also analyzed. In addition, ultrastructural alterations in leaf mesophyll and root tip cells were also analyzed in As-treated *B. napus* cultivars.

Materials and methods

Plant material and growth conditions

Seeds of two oilseed rape (*B. napus*) cultivars (ZS 758, and Zheda 622) which showed differences in tolerance against heavy metal (Farooq et al. 2015), were obtained from the College of Agriculture and Biotechnology, Zhejiang University. Mature seeds were treated with 70 % (v/v) ethanol for 3 min, transferred into 0.1 % (w/v) $HgCl_2$ for 8 min and then rinsed with deionized water until make sure that the $HgCl_2$ was completely washed out. The seeds were sown in plastic pots (170 × 220 mm) filled with peat moss. At the five-leaf stage, morphologically uniform seedlings were selected and plugged into plate holes in plastic pots (five plants per pot) containing a half-strength Hoagland's nutrient solution (Hoagland and Arnon 1941) aerated continuously with an air pump, and kept in a greenhouse. The pH of the solution was maintained at 6.0. The light intensity was in the range of 250–350 μmol m^{-2} s^{-1}, temperature was 16–20 °C and the relative humidity was approximately 55–60 %. After 2 weeks of acclimatization, solutions were adjusted to desired arsenic (As) concentration (0, 50, 100 and 200 μM). Sodium arsenite ($NaAsO_2$) was used to maintain different As concentrations and treatments were replicated three times. The nutrient solution was renewed after every 4 days.

Morphological parameters

Fifteen days after treatment, plants were harvested and separated into leaves and roots. For measurement of plant biomass, five plants per treatment were weighed immediately after being harvested and then placed into an oven at 80 °C. The dried samples were weighed immediately after the removal from the oven until biomass become stable (Momoh and Zhou 2001).

Chlorophyll (Chl *a, b*) and carotenoid (Car) contents in leaves were determined according to the method of Porra et al. (1989).

Photosynthetic gas exchange parameters were measured after 14 days of treatment by LiCor-6400 portable photosynthesis system (Li-Cor Inc., Lincoln, NE, USA). Photosynthetic rate (Pn), stomatal conductance (gs), intercellular CO_2 concentration (ci), and transpiration rate (E) were determined on the top most fully expanded leaf after 2 h of acclimation in a growth cabinet, at a temperature of 18 °C under a light intensity of 1000 μmol m^{-2} s^{-1}, relative humidity of 60 %. Eight leaves per plant/replicate from each treatment were taken for measurement (Zhou and Leul 1999).

Fractionation of leaves, roots for As analysis

After completion of experiment, *B. napus* plants were harvested, rinsed with deionized water three times and carefully separated into shoots and roots. Fresh tissues (1 g) of stems and roots from each replication were collected for immediate separations of subcellular fractions. Separations of subcellular fractions were performed according to the method of Feng et al. (2011) with some modifications. Samples were homogenized using a pre-cooled mortar and pestle in a medium containing 20 mL grinding solution (pH 7.8) of 0.25 mM sucrose, 50 mM

Tris–maleate buffer (pH 7.8), 1 mM $MgCl_2$ and 10 mM cysteine. The fractionation processes were operated at a constant temperature of 4 °C. After homogenization, the homogenate was transferred into a 50 mL centrifuge tube and centrifuged at 300×*g* for 30 s (Eppendorf AG, model 2231, Hamburg, Germany). The residue in the centrifuge tube was collected as cell wall fraction (fraction I). The supernatant was carefully transferred into another clean centrifuge tube, and then again centrifuged at 20,000×*g* for 45 min at 4 °C (Eppendorf AG, model 2231, Hamburg, Germany). The residue of the second centrifugation step was taken as cell organelle (fraction II), and the resultant supernatant was designated as soluble fractions (fraction III). The different cell fractions obtained were oven-dried at 70 °C to constant weight, ashed at 500 °C for 12 h, and dissolved in 1:1 (v:v) HNO_3, then the subcellular fractions of As in *B. napus* leaves and roots were determined using an atomic fluorescence spectroscopy (model AFS-230E, Beijing Kechuang Haiguang Instrument Company, China).

Histochemical analyses

Hydrogen peroxide (H_2O_2) accumulation in leaves was visually detected as the appearance of brown spots after the staining with 3,3-diaminobenzidine (DAB) by using the method of Romero-Puertas et al. (2004). The superoxide ($O_2^{\bullet-}$) accumulation was visualized as the appearance of dark spots using the nitroblue tetrazolium (NBT) staining procedure (Romero-Puertas et al. 2004). NBT and DAB-stained leaves were photographed using a digital camera (Canon DS126201, Japan). While, NBT and DAB-stained roots were observed under a light microscope (model Leica MZ 95) by using the method of Thordal-Christensen et al. (1997).

Analysis of lipid peroxidation and reactive oxygen species (ROS)

Lipid peroxidation in the leaves and roots, measured in terms of malondialdehyde (MDA) concentration was analyzed according to Zhou and Leul (1999).

For determination of hydrogen peroxide (H_2O_2) concentrations, leaves and roots (0.5 g) were extracted with 5.0 mL of TCA (0.1 %, w/v) in an ice bath, and the homogenate was centrifuged at 12,000×*g* for 15 min (Eppendorf AG, model 2231, Hamburg, Germany) (Velikova et al. 2000). The 0.5 mL supernatant was mixed with 0.5 mL of 10 mM potassium phosphate buffer (pH 7.0) and 1 mL of 1 M KI was added. The absorbance was read at 390 nm and the H_2O_2 concentration was calculated by using a standard curve.

Superoxide radical ($O_2^{\bullet-}$) was determined according to Jiang and Zhang (2001) with some modifications. The samples of fresh leaf and root (0.5 g) were homogenized in 3 mL of 65 mM potassium phosphate buffer (pH 7.8) and then homogenate was centrifuged at 5000×*g* for 10 min at 4 °C (Eppendorf AG, model 2231, Hamburg, Germany). After that the supernatant (1 mL) were mixed with 0.9 mL of 65 mM potassium phosphate buffer (pH 7.8) and 0.1 mL of 10 mM hydroxylamine hydrochloride, and then incubated at 25 °C for 24 h. After incubation 1 mL of 17 mM sulphanilamide and 1 mL of 7 mM a-naphthylamine was mixed in 1 mL solution for further 20 min at 25 °C. After incubation, n-butanol in the same volume was added and centrifuged at 1500×*g* for 5 min. The absorbance in the supernatant was read at 530 nm. A standard curve was used to calculate the generation rate of $O_2^{\bullet-}$.

Total RNA extraction, cDNA synthesis, and quantitative real-time PCR (qRT-PCR) assays

Total RNA was extracted from approximately 100 mg of leaf and root tissues using manual (Trizol) method. Prime Script ™RT reagent with gDNA (genomic DNA) eraser kit (Takara Co. Ltd., Japan) was used to remove the genomic DNA and cDNA synthesis. The synthesized cDNA from different treatments was the template for quantitative real time PCR (qRT-PCR) in the iCycler iQTM Real-time detection system (Bio-Rad, Hercules, CA, USA) by using SYBR® Premix Ex Taq II (Takara Co. Ltd., Japan). Primers for selected genes were constructed by using primer tools such as vector NTI with the help of sequence databases provided by NCBI (National Center for Biotechnology Information) (http://www.ncbi.nlm.nih.gov). The sequences (5′ → 3′) of forward (F) and reverse (R) primers of each candidate genes were presented as follows;

Gene name	Accession number	Sequences of primers (5́—3́)
SOD	AF540558	F: ACGGTGTGACCACTGTGACT
		R: GCACCGTGTTGTTTACCATC
POD	DQ078754	F: ATGTTTCGTGCGTCTCTGTC
		R: TACGAGGGTCCGATCTTAGC
CAT	GQ500124	F: TCGCCATGCTGAGAAGTATC
		R: TCTCCAGGCTCCTTGAAGTT
APX	Y11461	F: ATGAGGTTTGACGGTGAGC
		R: CAGCATGGGAGATGGTAGG
GR	AF008441	F: AAGCTGGAGCTGTGAAGGTT
		R: AGACAGTGTTCGCAAAGCAG
HSP90	NM001247507	F: GCTGCTGGTGCTGATGTTAG
		R: AGGAAGAGGGTCATTTTGGT
MT	GU189581	F: TCTTGCTGTGGAGGAAACTG
		R: AGCCCAAGTCTGGGTACATC

Gene name	Accession number	Sequences of primers (5́—3́)
Actin gene	FJ529167	F: TTGGGATGGACCAGAAGG R: TCAGGAGCAATACGGAGC

The PCR conditions consisted of denaturation at 95 °C for 3 min, followed by 40 cycles of denaturation at 95 °C for 30 s, annealing at 58 °C for 45 s and finally extension at 72 for 45 s. System software calculated the CT (threshold cycle) for each reaction and further mRNA quantification was performed according to the method of Livak and Schmittgen (2001). The threshold cycle (Ct) value of actin was subtracted from that of the gene of interest to obtain ΔCt value.

Biochemical analysis of enzyme activities

For enzyme activity, samples (0.5 g) were homogenized in 8 mL of 50 mM potassium phosphate buffer (pH 7.8) under ice cold conditions. Homogenate was centrifuged at 10,000×*g* for 20 min at 4 °C (Eppendorf AG, model 2231, Hamburg, Germany) and the supernatant was used for the determination of the following enzyme activities. Total superoxide dismutase (SOD, EC 1.15.1.1) activity was determined with the method of Zhang et al. (2008) following the inhibition of photochemical reduction due to nitro blue tetrazolium (NBT). The reaction mixture was comprised of 50 mM potassium phosphate buffer (pH 7.8), 13 mM methionine, 75 µM NBT, 2 µM riboflavin, 0.1 mM EDTA and 100 µL of enzyme extract in a 3-mL volume. One unit of SOD activity was measured the amount of enzyme required to cause 50 % inhibition of the NBT reduction measured at 560 nm. Catalase (CAT, EC 1.11.1.6) activity was measured according to Aebi (1984) with the use of H_2O_2 (extinction coefficient 39.4 mM cm^{-1}) for 1 min at A_{240} in 3 mL reaction mixture containing 50 mM potassium phosphate buffer (pH 7.0), 2 mM EDTA-Na_2, 10 mM H_2O_2 and 100 µL enzyme extract. Peroxidase (POD, EC1.11.1.7) activity was assayed by Zhou and Leul (1999) with some modifications. The reactant mixture contained 50 mM potassium phosphate buffer (pH 7.0), 1 % guaiacol, 0.4 % H_2O_2 and 100 µL enzyme extract. Variation due to guaiacol in absorbance was measured at 470 nm. The assay for ascorbate peroxide (APX, EC 1.11.1.11) activity was measured in a reaction mixture of 3 mL containing 100 mM phosphate (pH 7), 0.1 mM EDTA-Na_2, 0.3 mM ascorbic acid, 0.06 mM H_2O_2 and 100 µL enzyme extract. The change in absorption was taken at 290 nm 30 s after addition of H_2O_2 (Nakano and Asada, 1981). Glutathione reductase (GR, EC 1.6.4.2) activity was assayed by Jiang and Zhang (2002) with the oxidation of NADPH at 340 nm (extinction coefficient 6.2 mM cm^{-1}) for 1 min. The reaction mixture was comprised of 50 mM potassium phosphate buffer (pH 7.0), 2 mM EDTA-Na_2, 0.15 mM NADPH, 0.5 mM GSSG and 100 µL enzyme extract in a 1 mL volume. The reaction was started by using NADPH.

Transmission electron microscopy

After 14 days, leaf fragments without veins and small sections of root tips (1–3 mm) in length were collected from randomly selected plants and then fixed overnight in 2.5 % glutaraldehyde (v/v) in 0.1 M PBS (sodium phosphate buffer, pH 7.4) and washed three times with the same PBS. Then the samples were post fixed in 1 % OsO_4 [osmium (VIII) oxide] for 1 h and washed three times in 0.1 M PBS (pH 7.4), with 10-min intervals between each washing. Samples were dehydrated in a graded series of ethanol (50, 60, 70, 80, 90, 95 and 100 %) with 15–20-min intervals and at the end washed by absolute acetone for 20 min. The samples were then infiltrated and embedded in Spurr's resin overnight. After heating at 70 °C for 9 h, ultrathin sections (80 nm) of specimens were prepared and mounted on copper grids for viewing by a transmission electron microscope (JEOLTEM-1230EX, Tokyo, Japan) at an accelerating voltage of 60.0 kV.

Statistical analysis

The data were analyzed using SPSS v16.0 (SPSS, Inc., Chicago, IL, USA). A two-way analysis of variance (ANOVA) was carried out, followed by the Duncan's multiple range tests.

Results

Effect of As stress on dry biomass

Higher dose (200 µM) of As stress significantly decreased leaf dry weight by 47 % (cv. ZS 758) and 68 % (Zheda 622) as compared to their respective controls; lower level of As (50 µM) did not show any significant effect in both *B. napus* cultivars (Table 1). Moreover, a significant decrease in root dry weight ($p \leq 0.05$) was recorded in both *B. napus* cultivars among the control and lower treatment but much more significant decrease was observed at higher As concentration. At 100 µM As, the decrease in dry weight was 18 %; while, at higher As (200 µM) 50 % decrease in root dry weight was observed in ZS 758. Similarly, in cultivar Zheda 622 root dry weight was reduced by 38 and 70 % under different concentrations (100 and 200 µM) of As respectively, as compared to control. This indicated that Zheda 622 was more susceptible to As-stress than ZS 758.

Table 1 Effect of different As concentrations (0, 50, 100 and 200 µM) on the plant biomass (g), photosynthetic pigments (mg g^{-1} FW) and photosynthetic parameters; net photosynthetic rate (µmol CO_2 m^{-2} s^{-1}), stomatal conductance (mol H_2O m^{-2} s^{-1}), intercellular CO_2 concentration (µmol CO_2 mol^{-1}) and transpiration rate (mol H_2O m^{-2} s^{-1}) of two *B. napus* cultivars (*ZS* 758 and Zheda 622)

Cultivar	As conc. (µM)	Dry biomass		Photosynthetic pigments			Photosynthetic parameters			
		leaf	Root	Chl *a*	Chl *b*	Carotenoids	Photosynthetic rate (Pn)	Stomatal conductance (gs)	Intercellular CO_2 conc.	Transpiration rate
ZS 758	0	7.86 ± 0.045a	3.28 ± 0.028a	13.5 ± 0.015a	10.47 ± 0.02b	5.11 ± 0.043a	7.19 ± 0.035b	2.41 ± 0.03a	246.4 ± 5.08a	3.26 ± 0.035a
	50	7.54 ± 0.047b	2.96 ± 0.111b	12.81 ± 0.071a	9.85 ± 0.067b	4.9 ± 0.025a	7.28 ± 0.025a	2.39 ± 0.02ab	253.47 ± 6.06a	3.24 ± 0.02a
	100	6.73 ± 0.065d	2.68 ± 0.051c	10.93 ± 0.06c	6.36 ± 0.024e	3.46 ± 0.023b	6.21 ± 0.025c	2.04 ± 0.025d	205.29 ± 3.15c	3.23 ± 0.064a
	200	4.06 ± 0.078f	1.72 ± 0.025e	9.87 ± 0.048d	5.45 ± 0.06f	2.56 ± 0.02d	5.33 ± 0.03e	1.89 ± 0.02e	181.22 ± 0.77d	2.12 ± 0.032d
Zheda 622	0	8 ± 0.055a	3.19 ± 0.037a	13.18 ± 0.015a	11.25 ± 0.04a	4.92 ± 0.068a	7.24 ± 0.015b	2.35 ± 0.03b	252.21 ± 5.63a	3.24 ± 0.02a
	50	7.80 ± 0.037ab	2.85 ± 0.04b	11.31 ± 0.034b	9.13 ± 0.04c	4.85 ± 0.101a	7.19 ± 0.01b	2.17 ± 0.025c	226.11 ± 6.61b	2.96 ± 0.062b
	100	5.57 ± 0.035e	1.97 ± 0.06d	7.79 ± 0.014e	5.08 ± 0.034g	2.77 ± 0.28c	5.56 ± 0.015d	1.82 ± 0.02f	165.63 ± 1.49e	2.78 ± 0.036c
	200	2.52 ± 0.055g	0.94 ± 0.049f	6.4 ± 0.037f	3.87 ± 0.025h	1.57 ± 0.030e	4.19 ± 0.02f	1.46 ± 0.05g	135.18 ± 3.63f	1.85 ± 0.065e

The data are mean ± SD from three replications and different letters within a column show significance difference at $p \leq 0.05$ according to Duncan's multiple range test

Effect of As stress on chlorophyll contents

The effect of As stress on Chl *a*, Chl *b*, and carotenoids in *B. napus* seedlings after 14 days of treatment is shown in Table 1. The Chl contents of *B. napus* seedlings were not significantly inhibited at lower concentration of As (50 µM), but decreased as the As concentration increased. Under 200 µM As, Chl *a* and *b* contents were strongly reduced by 51 % (Chl *a*), 65 % (Chl *b*) for Zheda 622, and 26 % (Chl *a*), and 47 % (Chl *b*) for ZS 758 as compared to their respective controls. Similar to Chl contents, no significant decrease in carotenoid contents at 50 µM of As was observed in both *Brassica* cultivars. At 200 µM As, decrease in carotenoid contents was 48 and 71 % in both cultivars ZS 758 and Zheda 622 respectively.

Effect of As stress on photosynthetic parameters

The As response to photosynthetic parameters of *B. napus* plants grown under different As concentrations is shown in Table 1. The As stress at 50 µM did not cause any significant difference in the photosynthetic parameters i.e., Pn and gs between both cultivars. However, increasing concentrations of As led to a significant effect on Pn rate. Pn rate in cultivar Zheda 622 was decreased by 22 and 41 % under different As concentrations (100 and 200 µM) respectively, as compared to ZS 758 (14 and 26 %). While in plants treated with 200 µM As, gs was lowered by 21 % for ZS 758 and 38 % for Zheda 622 as compared to control. By contrast, the intracellular CO_2 concentration (*Ci*) decreased linearly as we increased As concentration in nutrient solution, in both the cultivars. Lower levels of As (50 and 100 µM) did not show any significant change in transpiration rate in cultivar ZS 758; while, a decreasing trend was observed in Zheda 622 at these As levels as compared to control. However, the decrease in transpiration rate was more pronounced under 200 µM As level in both cultivars; but less decrease was observed in ZS 758 as compared to Zheda 622.

Subcellular distribution of As

The As contents deposition in subcellular fractions of cell wall, cell organelles and soluble fraction of roots and leaves and sum of all the fractions (FI, FII and FIII) have been presented in Table 2. Higher contents of As were found in root fractions of both cultivars as compared to leaves. In addition, higher contents of As was found in cell wall fractions of roots and leaves as compared to soluble fractions and cell organelles, respectively. In cultivar ZS 758, As contents in leaf cell wall and soluble fraction was 53 and 14 % respectively under 50 µM As, while at 200 µM treatment cell wall deposited 51 % and soluble

fraction deposited 28 % As as compared to the sum of As in fractions. In root, at lower concentration (50 μM) cell wall deposited about 42 % of As while the less deposition was observed in soluble fraction (33 %) as compared to sum of As in fractions deposition at 50 μM, meanwhile the deposition of As at higher concentration (200 μM) in the cell wall was 53 and 24 % for soluble fraction as compared to sum of As in fractions deposition at 200 μM. Similarly, in the leaves of Zheda 622 at 50 μM, cell wall and soluble fraction deposited 43 and 32 % As respectively, while at 200 μM cell wall deposited 35 % As higher than other cell organelles (17 %). In root at 50 μM, As deposition was 43 and 34 % in cell wall and soluble fraction respectively; while at 200 μM 53 and 23 % As was deposited in cell wall and soluble fraction respectively. Thus, a genotypic difference was noted in accumulation of As concentrations in different subcellular fractions. On average of four As levels, cultivar ZS 758 exhibited low As concentrations in the cell wall and soluble fraction of roots and leaves as compared to Zheda 622.

Histochemical detection

Histochemical staining of ZS 758 and Zheda 622 showed different responses to DAB and NBT at different As treatments. The production of $O_2^{\bullet -}$ in *B. napus* leaves was studied by infiltrating leaves with NBT staining which gave dark spots of blue formazan; while, staining of DAB was based on the formation of brown spots (Fig. 2). In both cultivars, NBT staining of leaves treated with 50 μM As revealed no remarkable differences as compared to control (Fig. 1). Yet with the increased concentration of As, more dark spots of blue formazan were observed in leaves of both cultivars. In the similar way, higher accumulation of hydrogen peroxide (H_2O_2) was observed in cultivar Zheda 622 than ZS 758 plants, particularly at 200 μM of As treatment as revealed by brown spots formation in the leaves (Fig. 2). While, in case of root the blue formazan and brown color on the root tip was darker with the increase of As concentrations. Meanwhile, the comparison among cultivars revealed that the production of superoxide radical ($O_2^{\bullet -}$) was more in cultivar Zheda 622 as compared to ZS 758.

Lipid peroxidation (MDA) and reactive oxygen species (ROS)

Lipid peroxidation in terms of MDA contents was measured in *B. napus* plants exposed to As stress (Fig. 3a). No significant difference was observed in MDA contents at lower concentration of As as compared to control. The accumulation of MDA contents was increased significantly

Table 2 Effect of different As concentrations (0, 50, 100 and 200 μM) on arsenic concentration in subcellular fractions of roots and leaves of two *B. napus* cultivars (ZS 758 and Zheda 622)

Cultivar	As conc. (μM)	As in leaf fractions (mg kg^{-1} FW)				As in root fractions (mg kg^{-1} FW)			
		Cell wall (FI)	Cell organelles (FII)	Soluble fraction (FIII)	Sum of As in fractions	Cell wall (FI)	Cell organelles (FII)	Soluble fraction (FIII)	Sum of As in fractions
ZS 758	0	0.29 ± 0.07e	0.1 ± 0.04h	0.98 ± 0.08e	1.37 ± 0.04f	5.73 ± 0.17g	4.41 ± 0.11f	14.03 ± 3.64e	24.17 ± 2.02g
	50	4.5 ± 0.45d	2.25 ± 0.18f	1.2 ± 0.04e	7.95 ± 0.22e	77.93 ± 0.07f	41.38 ± 4.82e	64.7 ± 4.13d	184.01 ± 3.02f
	100	5 ± 0.59d	2.89 ± 0.12e	3.34 ± 0.12d	11.23 ± 0.09d	296.36 ± 29.95d	95 ± 12.25d	135 ± 2.51c	526.36 ± 7.52d
	200	13.11 ± 0.3b	5.13 ± 0.21b	7.28 ± 0.13a	25.52 ± 0.11b	518.3 ± 9.50b	141.45 ± 10.05c	205.66 ± 11.04b	865.41 ± 4.63b
Zheda 622	0	0.34 ± 0.13e	0.33 ± 0.05g	0.35 ± 0.36f	1.27 ± 0.07f	10.89 ± 0.21g	7.41 ± 0.08f	22.22 ± 2.14e	40.52 ± 5.5g
	50	4.97 ± 0.28d	3.05 ± 0.04d	3.78 ± 0.12c	11.8 ± 0.14d	178.89 ± 8.53e	78.8 ± 9.69d	132.5 ± 11c	390.19 ± 25.34e
	100	8.72 ± 1.02c	3.56 ± 0.07c	5.42 ± 0.14b	17.7 ± 0.16c	341.2 ± 17.39c	174.21 ± 13.42a	225 ± 12.01b	740.41 ± 10.34c
	200	22.01 ± 2.22a	10.78 ± 0.09a	7.03 ± 0.07a	39.82 ± 1.17a	683.7 ± 20.68a	147.73 ± 11.84b	335.9 ± 10.53a	1167.33 ± 12a

The data are mean ± SD from three replications and different letters within a column show significance difference at $p \leq 0.05$ according to Duncan's multiple range test

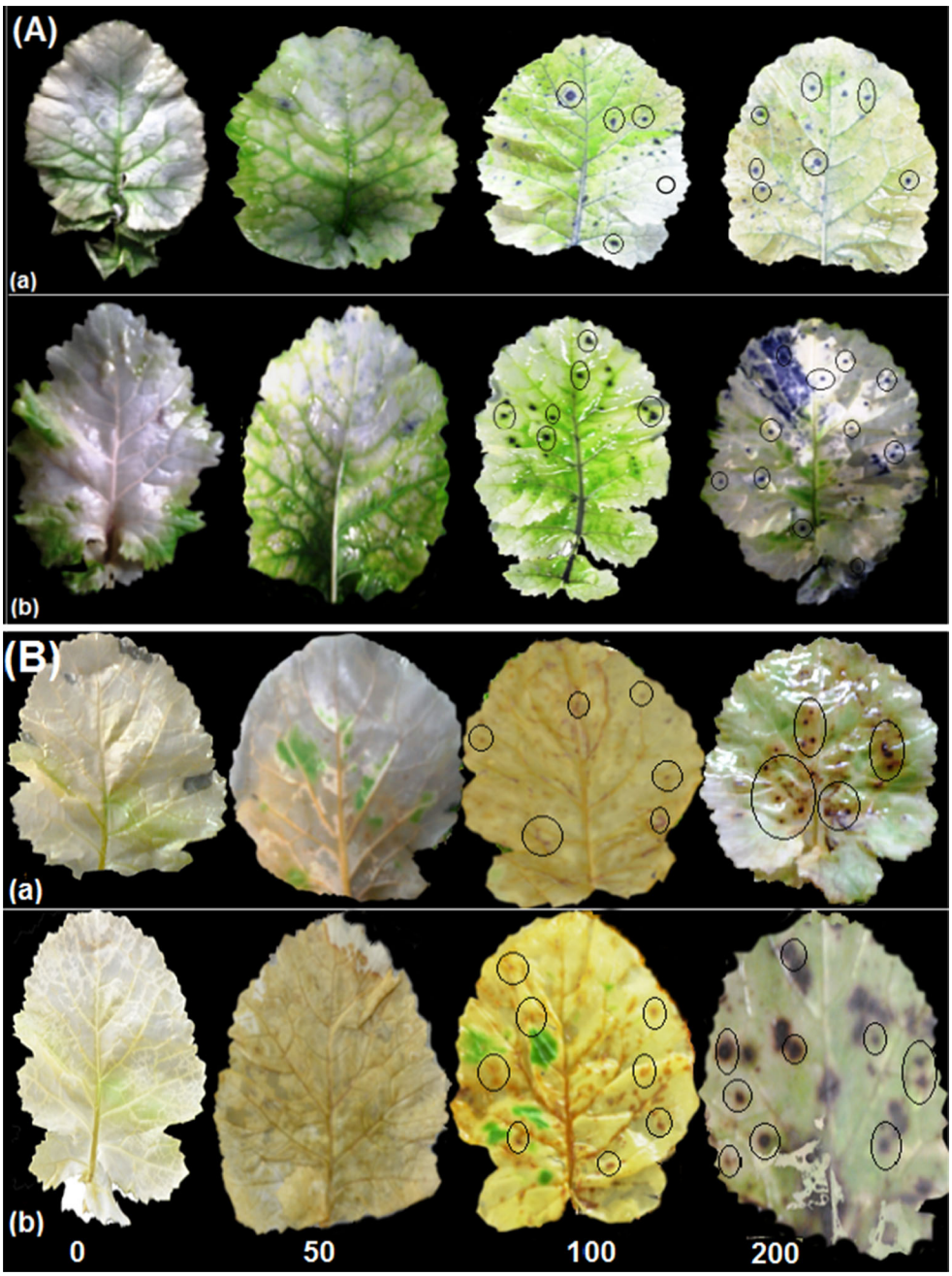

Fig. 1 Histochemical detection of superoxide ($O_2^{\bullet-}$) and hydrogen peroxide (H_2O_2) in leaves was performed by nitroblue tetrazolium (NBT) and 3,3-diaminobenzidine (DAB) staining, respectively. **A** Represents the $O_2^{\bullet-}$ accumulation for the *B. napus* leaves *a* ZS 758 and *b* Zheda 622; and **B** represents the H_2O_2 accumulation in *B. napus* leaves *a* ZS 758 and *b* Zheda 622

in the roots and leaves of both cultivars when treated with 200 μM As and more obvious in Zheda 622.

The extent of oxidative stress caused by As stress can also be demonstrated by ROS concentrations (Fig. 3b, c). The H_2O_2 and $O_2^{\bullet-}$ concentration in the roots and leaves of both cultivars increased when the plants were exposed to higher As concentration as compared to respective controls. The $O_2^{\bullet-}$ concentration in root at 50 μM As was not significantly different from the control plants in cultivar ZS 758 but increased significantly in Zheda 622 (Fig. 3b). Meanwhile, as we increased As concentrations (100 and 200 μM), significant effect was observed in the roots of both cultivars. While, for leaves the $O_2^{\bullet-}$ concentration was significantly increased at all As levels. Similarly for H_2O_2 contents no significant difference was observed in the leaves of cultivar ZS 758 at 50 μM As level, but increased in Zheda 622 (Fig. 3c). Similarly, for roots enhanced concentration of H_2O_2 was observed at all As levels and

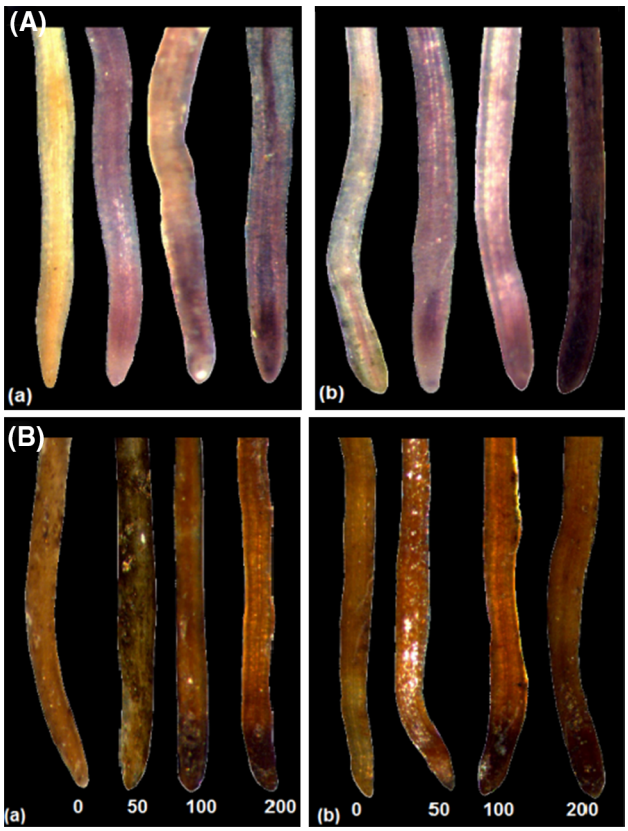

Fig. 2 Histochemical detection of superoxide ($O_2^{\bullet-}$) and hydrogen peroxide (H_2O_2) in roots was performed by nitroblue tetrazolium (NBT) and 3,3-diaminobenzidine (DAB) staining, respectively. **A** Represents the $O_2^{\bullet-}$ accumulation in *B. napus* roots of *a* ZS 758 and *b* Zheda 622; and **B** represents the H_2O_2 accumulation in *B. napus* root tips of *a* ZS 758 and *b* Zheda 622

maximum contents were found at 200 μM As, however the effect was more obvious in cultivar Zheda 622 (Fig. 3c).

Antioxidant enzymes response to As stress

Activities of SOD and GR in leaves and roots of both cultivars were enhanced as we increased As concentrations in solution (Table 3). At lower 50 μM As, a marked enhancement in SOD while slight change in GR activity was observed in both leaves and roots. At 100 or 200 μM As, both cultivars showed higher contents of SOD and GR activities. In general, SOD and GR activities in both roots and leaves were increased with the increasing concentration of As in medium. Among the cultivars, ZS 758 had higher SOD and GR activities in both leaves and roots than Zheda 622 (Table 3). Moreover, no significant difference was observed in leaf APX activity of cultivar ZS 758 at 50 μM As but slight increase was found in Zheda 622 as compared to control. However, a significant increase in APX activity was recorded with increasing As concentrations (100 and 200 μM). While in roots, significant increase in APX activity was observed at all treatment in case of cultivar ZS 758. While in roots, APX activity was increased in Zheda 622 at 50 μM As; whereas, at higher concentrations of As (100 and 200 μM), APX activity was gradually decreased in Zheda 622 (Table 3).

The CAT activity showed differential trend under As stress (Table 3). In the leaves, at 50 and 200 μM As, CAT activity was increased in both cultivars. However, at 100 μM CAT activity showed no significant change as compared to control plants. While in the roots, CAT activity was reduced in As treated plants in both cultivars as compared to control. In comparison to cultivars and treatments for ZS 758, no significant change was found in CAT activity, while for Zheda 622, at 50 and 100 μM As concentrations, CAT did not show any significant change as compared to control, but at higher 200 μM As level, CAT activity was decreased significantly. The POD activity in leaves and roots of control plants was higher as compared to As treated plants in both cultivars. In As treated plants, POD activity showed no remarkable difference at 50 and 100 μM As concentration. However, at higher As concentration (200 μM), a significant difference was recorded in POD activity (Table 3).

Antioxidant gene expression

The qRT-PCR analysis indicated that SOD and APX transcript levels of leaves were slightly increased at higher As level in both cultivars (Fig. 4a, b) as compared to their respective control. By contrast, in root the highest response of SOD and APX gene was noticed at 100 μM and then gradual decrease was observed at 200 μM in cultivar ZS 758. While the cultivar Zheda 622 showed similar pattern for SOD gene expression in root but no significance difference was observed for APX gene at higher levels (100 and 200 μM). The expression of CAT gene in leaf did not show any significant change under lower As levels (50 and 100 μM), but at higher As level (200 μM) an enhanced CAT gene expression was observed as compared to control (Fig. 4c). While, CAT gene in root did not show any expressional difference at all levels of As stress. However, the response of SOD, APX and CAT gene expression in leaves and roots of both cultivars were higher as compared to their respective control. In addition, cultivar ZS 758 had significantly higher SOD, CAT and APX gene expression than Zheda 622. Moreover, no significance difference was found in the gene expression of root POD at 50 μM As as compared to control and then down-regulated at higher As levels (100 and 200 μM). Similarly, in leaves no significant alteration was observed in POD gene expression at 50 μM as compared to control. Moreover, at 200 μM As level, leaves of cultivar ZS 758 showed higher transcript levels as compared to Zheda 622 where the POD gene expression

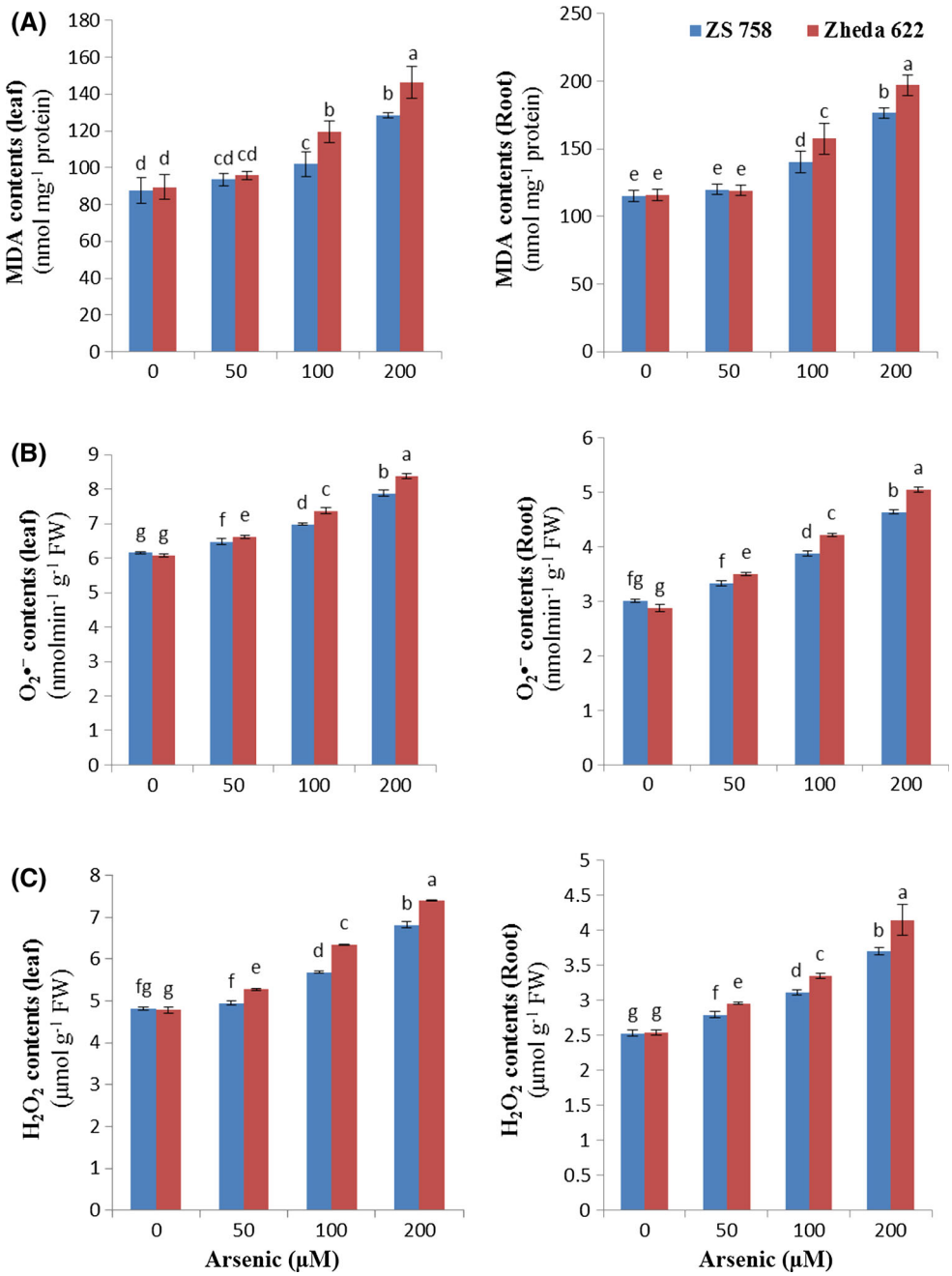

Fig. 3 Effect of different arsenic (As) concentrations on **A** lipid peroxidation (MDA), **B** superoxide ($O_2^{\bullet-}$) and **C** hydrogen peroxide (H_2O_2) in leaves and roots of two *B. napus* cultivars. *Vertical bars* represent mean ± SD. *Different letters* indicate statistically significant differences ($p \leq 0.05$) by applying Duncan's multiple range test

was down-regulated as we increased As concentration. The transcript level of GR in leaves was increased as we increased As concentration in solution as compared to control plants. No significant difference was observed in transcript level of leaf GR in cultivar ZS 758 at 50 and 100 µM As levels, however higher concentration (200 µM) of As significantly increased the GR gene expression (Fig. 4E). While for Zheda 622 leaves, slight decrease at 100 µM As was observed as compared to 50 µM As level but an increased transcription level was obtained at 200 µM As level. Further, slightly enhanced transcript level of root GR was found at 50 and 100 µM As levels; whereas transcript level was significant at 200 µM As in both cultivars as compared to their respective controls.

Ultrastructure changes in response to As stress

The ultrastructural changes in leaf mesophyll and root tip cells in control and As treated (200 µM) plants have been shown in Figs. 5 and 6. A clear and smooth cell wall with a well-organized chloroplast can be found in the leaf micrograph (Fig. 5). In the micrograph of control leaf, a well-developed chloroplast with properly arranged thylakoids as well as plastoglobuli and round mature mitochondria can

Table 3 Effect of different As concentrations (0, 50, 100 and 200 µM) on antioxidant enzymes; SOD (U g^{-1} FW), ascorbate peroxidase (APX), catalase (CAT), guaiacol peroxidase (POD), and glutathione reductase (GR) activities (µmol min^{-1} mg^{-1} protein) in the leaves and roots of two *B. napus* cultivars (ZS 758 and Zheda 622)

Cultivar	As conc. (µM)	SOD		APX		CAT		POD		GR	
		Leaf	Root	leaf	Root	Leaf	Root	Leaf	Root	leaf	Root
ZS 758	0	455.30 ± 15.01h	318.76 ± 1.5f	3.01 ± 0.025g	1.36 ± 0.03f	1.19 ± 0.02d	0.95 ± 0.04a	2.07 ± 0.015b	0.037 ± 0.001a	4.58 ± 0.077g	2.45 ± 0.02f
	50	667.67 ± 5.13g	619.61 ± 5.11c	3.04 ± 0.025 fg	1.58 ± 0.036c	1.42 ± 0.03b	0.83 ± 0.05bc	2.07 ± 0.020b	0.033 ± 0.003ab	5.05 ± 0.045e	2.95 ± 0.04e
	100	776.47 ± 4.69c	723.96 ± 5.46b	4 ± 0.02c	1.65 ± 0.03b	1.18 ± 0.03d	0.85 ± 0.02b	2.09 ± 0.011ab	0.033 ± 0.003ab	5.87 ± 0.032c	3.80 ± 0.061c
	200	868 ± 3.61a	792.81 ± 5.75a	4.96 ± 0.041a	1.74 ± 0.04a	1.46 ± 0.04a	0.81 ± 0.03bc	1.97 ± 0.020d	0.025 ± 0.001c	6.49 ± 0.04a	4.87 ± 0.05a
Zheda 622	0	494.39 ± 12.02g	295.96 ± 7.95g	2.98 ± 0.015g	1.29 ± 0.02g	1.18 ± 0.02d	0.92 ± 0.03a	2.11 ± 0.015a	0.035 ± 0.002a	4.61 ± 0.036g	2.50 ± 0.035f
	50	611.21 ± 16.86f	537.73 ± 3.63e	3.14 ± 0.02e	1.58 ± 0.04c	1.29 ± 0.02c	0.77 ± 0.013d	2.04 ± 0.01c	0.03 ± 0.002b	4.88 ± 0.035f	3.00 ± 0.047e
	100	724.27 ± 4.71d	587.78 ± 12.94d	3.64 ± 0.04d	1.51 ± 0.034d	1.17 ± 0.05d	0.78 ± 0.015d	2.08 ± 0.005ab	0.035 ± 0.003a	5.79 ± 0.03d	3.5 ± 0.05d
	200	801.68 ± 13.17b	626.03 ± 6.36c	4.58 ± 0.035b	1.42 ± 0.036e	1.31 ± 0.02c	0.67 ± 0.010e	1.92 ± 0.025e	0.022 ± 0.002d	6.02 ± 0.04b	4.42 ± 0.064b

The data are mean ± SD from three replications and different letters within a column show significance difference at $p \leq 0.05$ according to Duncan multiple range test

also been observed in control plants in both cultivars (Fig. 5a, b). However, at 200 µM As cell structure of both cultivars displayed fewer changes over their respective controls (Fig. 5). Swelling of the chloroplast with a large starch granule could be seen in cultivar ZS 758. More pronounced modification in ultrastructure features of the leaf mesophyll cells was noticed in Zheda 622 where considerable increase in the number of lipid bodies was observed. Thylakoids structures were become obscured and unsmooth (Fig. 5d). TEM micrographs of root tip cells of both cultivars at control showed no distortion in cell organelles, briefly having well developed nucleus with nucleolus and nuclear membrane. The fine structure of root tip tissue having clear mitochondria with smooth and continuous cell wall was observed at control conditions in both cultivars (Fig. 6a, b). However, at 200 µM As level, symptoms were clear in most of the organelles and significant changes in the root tip cells were observed in both cultivars (Fig. 6c, d). In Zheda 622, cellular set up was badly injured where the shrinkage of cell membrane, nucleolus disappearance and disruption of the nucleus and nuclear membrane could also be found in the cells of As-treated plants (Fig. 6d). However, least damaged was observed at this level in cultivar ZS 758 (Fig. 6c).

Expression of stress-related genes

Hsps are useful biomarkers because their induction is much more sensitive to stress and plays important role in protection and repair of protein folding under stress conditions. While MTs protect plants from metal stresses as they were proposed to function in both metal chaperoning and scavenging of ROS. Transcript levels of *Hsp*-90 and *MT* were detected by qRT-PCR under different concentrations of As (Fig. 7). In control leaves, transcript levels of these two genes underwent no significant changes in both cultivars but a slight increase was observed at lower concentration of As as compared to control. At higher concentration of As, the transcript levels of two genes were increased significantly in both cultivars. Furthermore, it was also observed that the transcript levels of *Hsp90* and *MT* were enhanced promptly upon all the concentrations of As in roots, and maximum induction was found at 200 µM As level. The induction of *MT* transcript level was obvious in the leaves and roots of cultivar ZS 758 than Zheda 622.

Discussion

Lately, the environmental fate and As behavior have received serious concern in South-East Asia countries due to its increasing amount in the environment. Arsenic has no known essential function in plant growth and generally

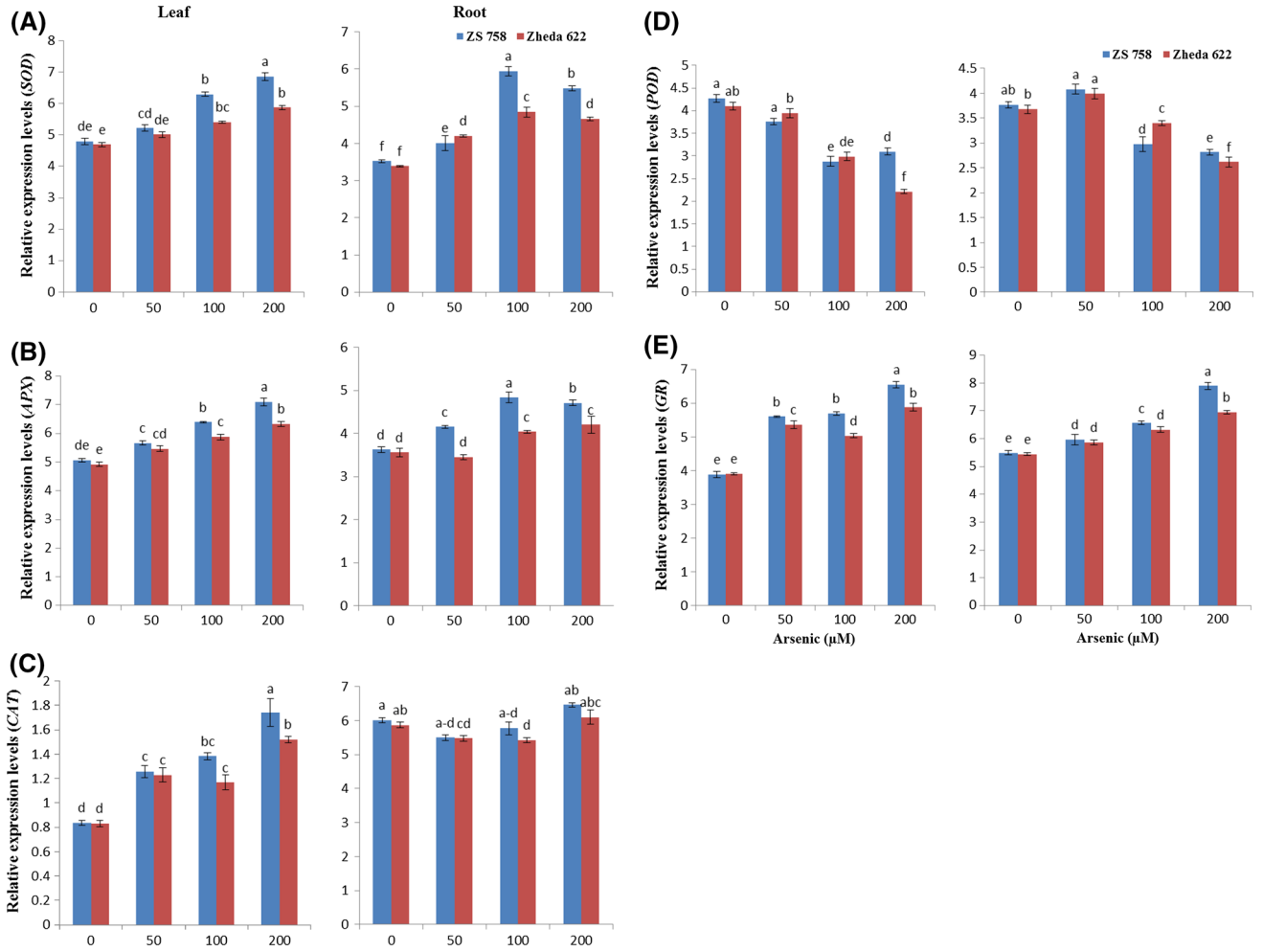

Fig. 4 Effect of different arsenic (As) concentrations on antioxidant related transcripts of superoxide dismutase (*SOD)* (**A**), ascorbate peroxidase (*APX)* (**B**), catalase (*CAT*) (**C**), guaiacol peroxidase *(POD)* (**D**), and glutathione reductase (*GR*) (**E**) in leaves and roots of two *B. napus* cultivars. *Vertical bars* represent mean ± SD from three CT values. *Different letters* indicate statistically significant differences ($p \leq 0.05$) by applying Duncan's multiple range test

causes damaging effects to the plant growth. In present study, various concentrations of As stress significantly reduced the biomass in both cultivars and this might be due to the toxic effect of As at higher concentrations (Table 1). Similar to the present study, a dose-dependent reduction in plant dry biomass was also reported by different investigators for rice (*O. sativa*) (Shri et al. 2009), wheat (*Triticum durum* L.) (Pigna 2009) and Indian mustard (*B. juncea)* (Ansari et al. 2013). The photosynthetic pigments are also sensitive physiological processes of plants that can also be affected by heavy metal stress. In this study, the contents of Chl *a, b* and carotenoids (Car) in As treated *B. napus* plants were decreased (Table 1). Loss in chlorophyll contents was in accordance with the findings of Mahdieh et al. (2013) who also found decline in chlorophyll and Car contents with As stress in wheat (*Triticum aestivum* L.) varieties. The decrease in the biosynthesis of Chl and Car related enzymes such as δ-aminolevulinic acid dehydratase (Jain and Gadre 2004) or reduction of rubisco activity might also be a possible reason for decrease of these pigments (Gusman et al. 2013). Meanwhile, the elevated concentration of As also decreased the photosynthesis (Table 2) due to their direct effect on the photosynthetic apparatus. The membrane systems of chloroplasts were found to be severely damaged by As exposure in *Pteris vittata* L. (Li et al. 2006). Moreover, Ahsan et al. (2010) also reported that in rice (*O. sativa*) leaves the photosynthetic metabolism related enzymes [(ribulose-1,5-bisphosphate carboxylase/oxygenase (Rubisco)] was found responsible for the decline in photosynthetic rate due to its down-regulation activity under As stress. Thus, higher As stress can induce changes in chloroplastic proteins and enzymes which might affect the photosynthetic efficiency of plants.

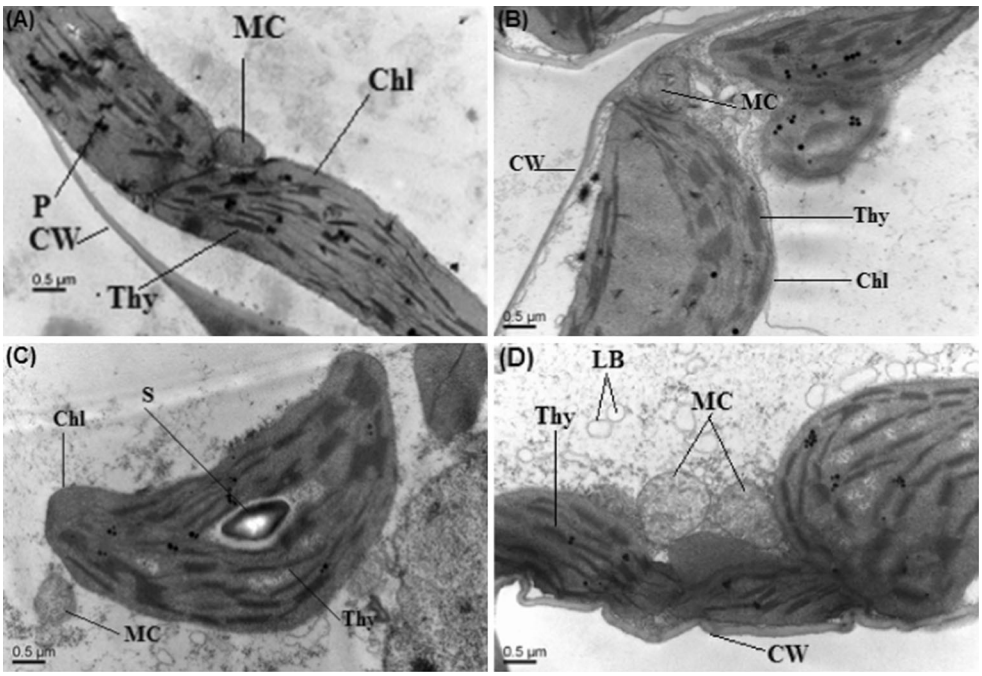

Fig. 5 Electron micrographs of leaf mesophyll of 14-days grown seedlings of two cultivars of *B. napus* (cvs. ZS 758 and Zheda 622) under control (CK) and arsenic (As) 200 µM concentration. **A** TEM micrograph of leaf mesophyll cells of ZS 758 under control (CK) shows well developed chloroplast (Chl), thylakoid membranes (Thy), plastoglobuli structures (P), mitochondria (MC) with clear cell wall (CW) and starch grain (S). **B** TEM micrograph of leaf mesophyll cells of Zheda 622 under control (CK) shows a clear cell wall (CW), chloroplast (Chl) with thylakoid membranes (Thy) and a rounded mitochondria (MC). **C** TEM micrograph of leaf mesophyll cells of ZS 758 under 200 µM As shows a well-developed chloroplast (Chl), starch grain (S), mitochondria (MC) and thylakoid (Thy). **D** TEM micrograph of leaf mesophyll cells of Zheda 622 under 200 µM As shows unsmooth cell well (CW) and unclear thylakoid membranes (Thy), and two large mitochondria (MC)

Plant species and genotypes significantly differ in the uptake of heavy metal and its subsequent translocation from roots into shoots (Meharg and Hartley-Whitaker 2002: Bhattacharya et al. 2013). In the present study, significant increase in As accumulation was observed in both *B. napus* cultivars after As treatments (Table 2). Moreover, cultivar Zheda 622 uptakes more As contents both in roots and leaves than ZS 758. The heavy metal distribution at cellular and subcellular levels significantly has greater importance for the detoxification and accumulation of heavy metals in plants (Zhou et al. 2010). The cell wall is considered as the first barrier for metal ion uptake into cells (Dronnet et al. 1996) and can bind divalent and trivalent metal cations and limits the quantity of metals entering the cytoplasm (Seregin and Ivanov 1997). Therefore, the cell wall acts as key storage compartment fractions of metal in plants (Megateli et al. 2009). Present study showed that As in *B. napus* plants were predominantly accumulated in the cell wall of roots (Table 2). However, some other studies reported different patterns of distribution such as in oilseed rape (*B. napus*) (Carrier et al. 2003) and rice (*O. sativa*) (Xiong et al. 2009), where the heavy metal was present predominantly in the soluble fraction. These differences may be attributed due to concentrations and species differences. Another heavy metal uptake study showed a similar As uptake mechanism in *P. vittata*, where As was mainly accumulated in the cell wall fraction of root (Liao et al. 2007). Further, Zeng et al. (2011) also observed that in rice (*O. sativa)* plants the highest concentration of heavy metal was found in the cell-wall fraction of roots and in the supernatant soluble fraction.

Lipid peroxidation is considered as an index of oxidative damage under abiotic stress (Sun et al., 2011). Enhancement of $O_2^{\bullet-}$ can produce the hydroxyl radical (H_2O_2), which in turn converts fatty acids to toxic lipid peroxides, causing damage to membrane lipids, proteins, and nucleic acids (Hossain et al. 2012). High rate of lipid peroxidation in As-treated plants could be due to high ROS production (Fig. 3), which attacks membrane lipid leading to ion leakage and membrane deterioration. The increase in MDA contents directly correlated with high ROS production and growth inhibition, indicating that As-induced ROS production was the primary cause of lipid peroxidation. Increased MDA at 100 or 200 µM As, accordingly, suggests that higher As concentrations stimulate the lipid peroxidation, that causes irreversible damage to tissue development and function. These findings are consistent with previous reports by Choudhury et al. (2011) for *O.*

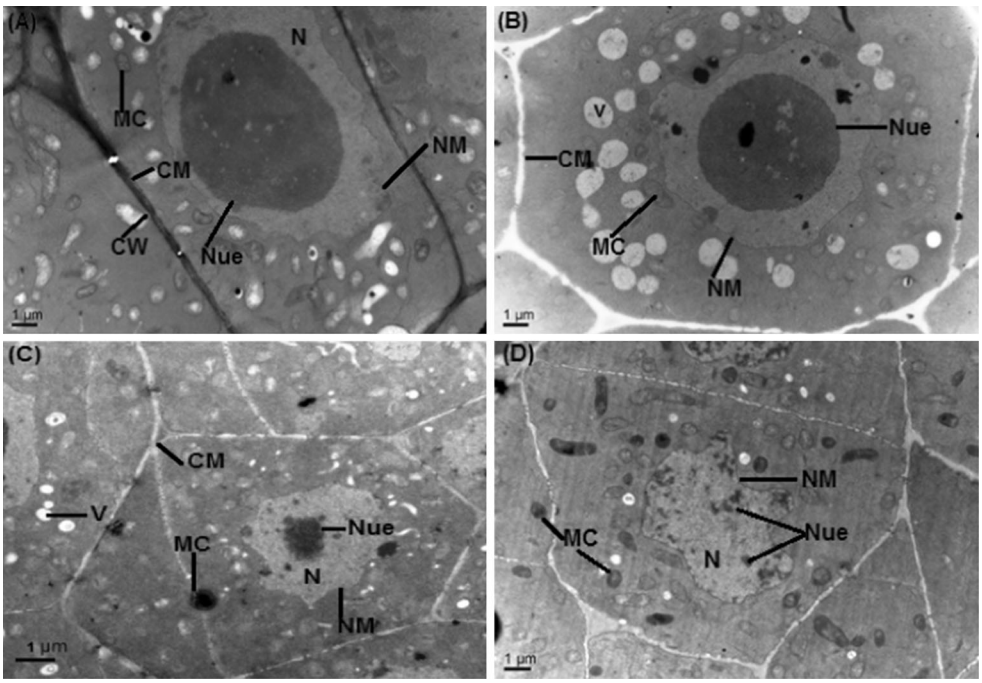

Fig. 6 Electron micrographs of root tip cells of 14-days grown seedlings of two cultivars of *B. napus* (cvs. ZS 758 and Zheda 622) under control (CK) and arsenic (As) 200 µM concentration. **A** TEM micrograph of root tip cells of ZS 758 under control (CK) shows a clear cell wall (CW) and cell membrane (CM), large nucleus (N) with number of nucleoli (Nue), nuclear membrane (NM) and mitochondria (MC). **B** TEM micrograph of root tip cells of Zheda 622 under control (CK) shows clear nucleus (N) with nucleoli (Nue), well developed mitochondria (M) and cell membrane (CM). **C** TEM micrograph of root tip cells of ZS 758 under 200 µM As shows scattered nucleus (N) with nucleoli (Nue), rounded mitochondria (MC) with Cell wall (CW) and small vacuoles (V). **D** TEM micrograph of root tip cells of Zheda 622 under 200 µM As shows damaged organelles such as nucleus (N) with nucleoli (Nue) and nuclear membrane (NM) and mitochondria (MC)

sativa, and Gupta et al. (2009) for *B. juncea* indicating that As stress induces lipid peroxidation resulting in the destruction of biological membranes. The increase in H_2O_2 and $O_2^{\bullet-}$ contents in root and shoots clearly indicated the As-induced ROS production (Fig. 3). At optimum level, ROS also acted as a secondary messenger in protein synthesis and gene expression but at elevated concentrations (100 or 200 µM As), ROS became cytotoxic (Foyer and Noctor 2005) and caused damage to the important organic constituent of the cells. A significant increase in $O_2^{\bullet-}$ and H_2O_2 contents may therefore have a less extensibility of plant cell walls, which can rapidly reduce the growth (Schutzendubel and Polle 2002). The $O_2^{\bullet-}$ and H_2O_2 formations under metal stress are supported by several recent reports (Feng et al. 2013; Gill et al. 2015; Farooq et al. 2015), and illustrate that the stability between formation and elimination of the active oxygen free radical is unbalanced in cells (Fridovich 1995), which would possibly result in cell death. As stress induced a significant accumulation of $O_2^{\bullet-}$ and H_2O_2 in *B. napus* cultivars leaves and roots and the extent of ROS production was more pronounced in Zheda 622 than ZS 758, these results were also verified by histochemistry with NBT and DAB staining (Figs. 1, 2). The level of H_2O_2 was lower in cultivar ZS 758 than Zheda 622 in the presence of As, which implied that the generation of H_2O_2 was quenched by the efficient antioxidative mechanism of ZS 758. In both *B. napus* cultivars, the level of H_2O_2 increased in a dose-dependent manner (Fig. 3c), and higher oxidative stress was observed on the plants when we increased As concentration. It is most likely that the presence of As inhibited the H_2O_2 scavenging enzyme and increased activity of SOD (Fig. 4a), which catalyzed the conversion of superoxide anion to $O_2^{\bullet-}$ and H_2O_2 (Verma and Dubey 2003). There was more pronounced increase in the SOD activity in cultivar ZS 758 than Zheda 622 with the increase in As levels. But H_2O_2 production was higher in cultivar Zheda 622 which was probably due to inactivation of CAT enzyme. That resulted in the accumulation of H_2O_2 in the cell as shown in Figure (Fig. 3c). In ROS detoxification process, SOD the first enzyme converts $O_2^{\bullet-}$ radicals to H_2O_2. The accumulation of further H_2O_2 is prevented by APX, CAT and POD. As a result of SOD reaction the increase in H_2O_2 was accompanied by enhanced enzymes activities to decompose it. Thus, CAT and APX coordinate with SOD and play an important role in scavenging the H_2O_2. Previous reports showed that treatment with As increased the specific activities of SOD, APX, and CAT

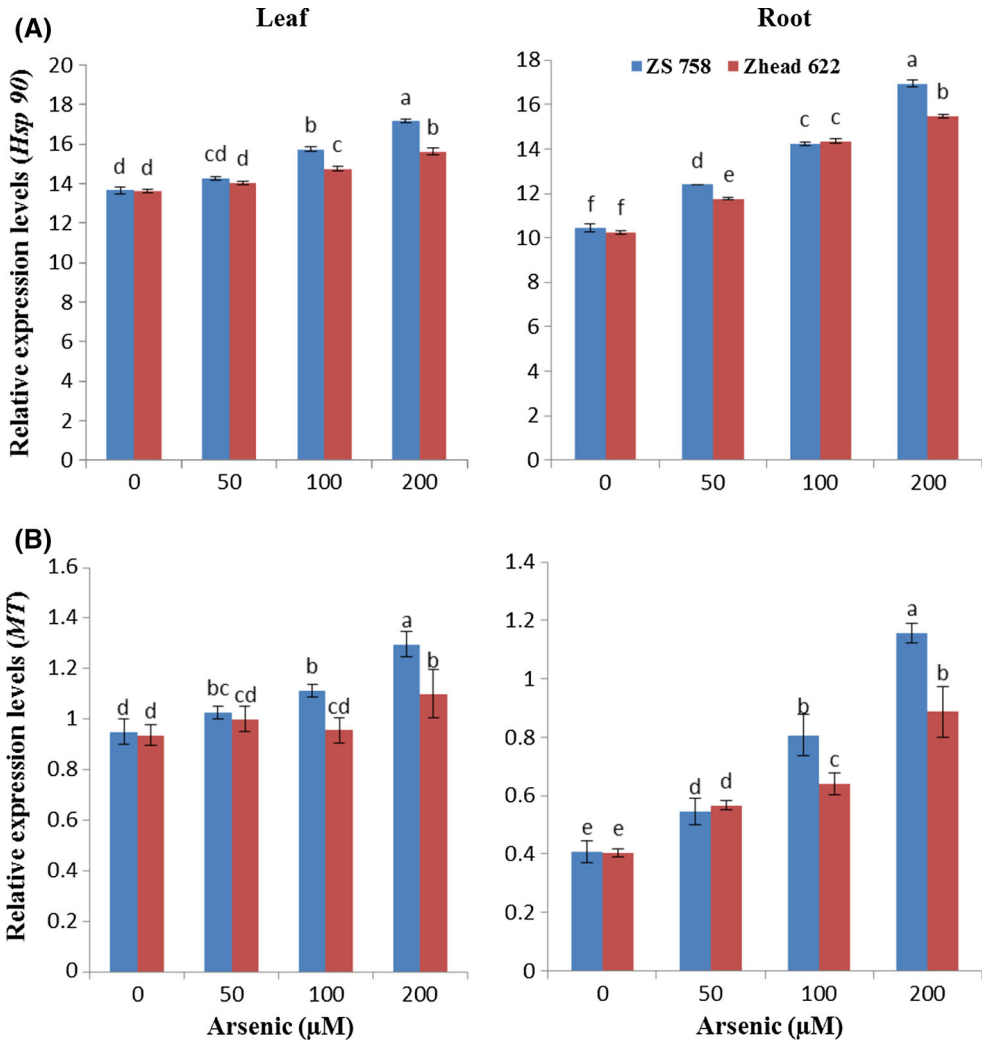

Fig. 7 Effect of different As concentrations on gene expression of heat shock protein 90-1 (Hsp90-1) (**A**), and metallothionein (MT) (**B**) in leaves and roots of two *B. napus* cultivars. *Vertical bars* represent mean ± SD from three CT values. *Different letters* indicate statistically significant differences ($p \leq 0.05$) by applying Duncan's multiple range test

in O. *sativa* (Shri et al. 2009), *B. juncea* (Gupta et al. 2009) and *T. aestivum* (Chun et al. 2007). The increased SOD, APX, and CAT activities show that these two plant cultivars have the ability to adapt As induced stress by developing an antioxidant defense system. Srivastava et al. (2006) reported that the accumulation of ROS under stress conditions signaled an increase in APX and GR activities, which in turn protected the plants from oxidative stress caused by As. Compared to those in Zheda 622, enhanced enzyme activities were more pronounced in cultivar ZS 758, whereas As-induced lipid peroxidation was lower, indicating that ZS 758 was more tolerant to As. In addition to these findings we also measured the gene expression of these antioxidant enzymes and the result was also in line with the activities of antioxidant enzymes. The transcript study of enzymes showed that the activities of SOD, APX, CAT, and GR were increased significantly in tolerant cultivar (ZS 758) in response to As stress, while sensitive cultivar (Zheda 622) showed a significant reduction in APX, POD and GR activities at different As treatments. Similar to these results, Panda and Matsumoto (2010) also suggested that tolerant cultivar had higher expression level of SOD, APX, CAT and GR under aluminum stress. While, similar gene expression phenomena was also studied under different metals stress like cadmium (Luo et al. 2011), copper (Rout and Sahoo 2013) and aluminum (Panda and Matsumoto 2010). The up-regulation of these different types of genes suggested their involvement in defense mechanism under As induced oxidative stress that exhibited the As-tolerance in *B. napus* cultivars.

In our present study, the cellular response of As-stress on two *B. napus* cultivars was also analyzed. Changes in different organelles of leaf and root cells were found as concentration-dependent. However, cultivar Zheda 622 was proved to be more affected as compared to ZS 758 (Fig. 5c, d). Recently, similar findings were also observed under cadmium and chromium stress in *B. napus* plants (Ali et al. 2014; Gill et al. 2015), and was concluded that higher concentrations of heavy metals damaged the cellular functioning of plants. Similarly, TEM analysis in present

study showed that higher concentration of As (200 μM) severely damaged the cellular structures of both *B. napus* cultivars. Disorders in cell structure as well as damages in different organelles were some of the obvious variations in cultivar Zheda 622 as compared to ZS 758 (Fig. 6c, d). These findings are also in accordance with the previous reports of Li et al. (2006) and Liao et al. (2007) which prove that higher concentrations of heavy metals can damage the cell organelles in the leaves and roots of plants.

Transcript levels of stress responsive genes were assessed by quantitative real-time PCR using RNAs isolated from roots and leaves of hydroponically cultivated *B. napus* plants. Exposure of *B. napus* plants to As led to dramatic changes in the abundance of stress-related transcripts, Hsp90-1 and MT-1 (Fig. 7). Hsps are proteins and useful biomarkers that play important roles in maturation and/or activation of over 100 'client proteins' involved in the processes of signal transduction and transcriptional regulation (Brown et al. 2007). In our study, As stress induced the expression of molecular chaperone *Hsp90* protein gene in both leaves and roots. Both the cultivars sensed the metallic stress and responded to As stress by activating the mechanisms to prevent the cellular homeostasis through alleviating the protein damage. The transcription accumulation was also reported under some other metal ion stresses such as cadmium and chromium (Goupil et al. 2009; Milioni and Hatzopoulos 1997). Moreover, Wang et al. (2010) proposed that MTs were involved in the function of both metal chaperoning and scavenging of ROS. They have ability to bind with heavy metals through their cysteine residue thiol groups. Previous studies showed that As and Cd stress induced metalloprotein expression and accumulation in plants (Goupil et al. 2009). It was observed that As treatment induced *MT*-like protein encoding gene transcription in roots and leaves of both cultivars and most of the accumulation was observed in the roots of ZS 758 at higher concentration (Fig. 7b). Ahn et al. (2012) reported that three MT genes *BrMT1, BrMT2,* and *BrMT3* were differentially regulated under various heavy metal stresses in *Brassica rapa* L. These findings show that metallothionein binding protein transcript accumulation induces As-stress tolerance in *B. napus* plants as it has lately shown in boron, arsenic and copper stresses (Tombuloglu et al. 2012; Goupil et al. 2009; Wang et al. 2010).

Conclusion

In conclusion, the present work studied the subcellular distribution of arsenic (As) and the physiological responses of *B. napus* at elevated concentrations of As. It was found that As stress decreased plant growth and photosynthetic parameters. As stress induced inhibition of photosynthesis to be attributed as reduction in photosynthetic pigments; decline in gas exchange parameters and mainly the damage of the photosynthetic apparatus. It's also found that there was a significant difference in As subcellular distribution and large amount of As was bound with the cell well. Further, As treatment caused obvious oxidative damage as evident in enhanced level of MDA. The level of ROS was lower in cultivar ZS 758 than Zheda 622 in all treatments. The differential responses of the antioxidant enzymes to As stress, both enzymatic and gene levels indicate that antioxidant activities can play predominant role in protection against oxidative stress induced by As stress in both cultivars (ZS 758 and Zheda 622). Further research is needed to identify important candidate genes and markers linked to As tolerance that can be applied to the genetic improvement of plants for enhanced As tolerance.

Acknowledgments This study was supported by the National High Technology Research and Development Program of China (2013AA103007), Jiangsu Collaborative Innovation Center for Modern Crop Production, Special Fund for Agro-scientific Research in the Public Interest (201303022), the Science and Technology Department of Zhejiang Province (2012C12902-1), and China Postdoctoral Science Foundation (2015M570512).

Compliance with ethical standards

Conflict of interest The authors declare that the research was conducted in the absence of any potential conflict of interest.

References

Aebi H (1984) Catalase in vitro. Methods Enzymol 105:121–126

Ahammed GJ, Choudhary SP, Chen S, Xia X, Shi K, Zhou Y, Yu J (2013) Role of brassinosteroids in alleviation of phenanthrene-cadmium co-contamination-induced photosynthetic inhibition and oxidative stress in tomato. J Exp Bot 64:199–213

Ahn O, Kim SH, Lee J, Kim HR, Lee HS, Kwak SS (2012) Three *Brassica rapa* metallothione in genes are differentially regulated under various stress conditions. Mol Biol Rep 39:2059–2067

Ahsan N, Lee DG, Kim KH, Alam I, Lee SH, Lee KW, Lee H, Lee BH (2010) Analysis of arsenic stress-induced differentially expressed proteins in rice leaves by two dimensional gel electrophoresis coupled with mass spectrometry. Chemosphere 78:224–231

Ali B, Qian P, Jin R, Ali S, Khan M, Aziz R, Tian T, Zhou WJ (2014) Physiological and ultra-structural changes in *Brassica napus* seedlings induced by cadmium stress. Biol Plant 58:131–138

Ansari MKA, Shao HB, Umar S, Ahmad A, Ansari HS, Iqbal M, Owens G (2013) Screening Indian mustard genotypes for phytoremediating arsenic-contaminated soils. Clean Soil Air Water 41:195–201

Austruy A, Wanat N, Moussard C, Vernay P, Joussein E, Ledoigt G, Hitmi A (2013) Physiological impacts of soil pollution and arsenic uptake in three plant species: *Agrostis capillaris*, *Solanum nigrum* and *Vicia faba*. Ecotoxicol Environ Safe 90:28–34

Bhattacharya P, Samal AC, Majumdar J, Banerjee S, Santra SC (2013) In-vitro assessment on the impact of soil arsenic in the

eight rice varieties of West Bengal, India. J Hazard Mater 262:1091–1097
Brown MA, Zhu L, Schmidt C, Tucker PW (2007) Hsp90: from signal transduction to cell transformation. Biochem Biophys Res Commun 363:241–246
Caldelas C, Bort J, Febrero A (2012) Ultrastructure and subcellular distribution of Cr in *Iris pseudacorus* L. using TEM and X-ray microanalysis. Cell Biol Toxicol 28:57–68
Carrier P, Baryla A, Havaux M (2003) Cadmium distribution and microlocalization in oilseed rape (*Brassica napus*) after long-term growth on cadmium contaminated soil. Planta 216:939–950
Choudhury B, Chowdhury S, Biswas AK (2011) Regulation of growth and metabolism in rice (*Oryza sativa* L.) by arsenic and its possible reversal by phosphate. J Plant Int 6:15–24
Chun L, Shu F, Yun S, Li J, Yang LX, Xiao H (2007) Effects of arsenic on seed germination and physiological activities of wheat seedlings. J Environ Sci 19:725–732
Dronnet VM, Renard C, Axelos MAV, Thibault JF (1996) Heavy metals binding by pectins: selectivity, quantification and characterisation. In: Visser J, Voragen AGJ (eds) Pectins and pectinases, vol 14. Elsevier, Amsterdam, pp 535–540
Farooq MA, Li L, Ali B, Gill RA, Wang J, Ali S, Gill MB, Zhou WJ (2015) Oxidative injury and antioxidant enzymes regulation in arsenic-exposed seedlings of four *Brassica napus* L. cultivars. Environ Sci Pollut Res 22:10699–10712
Feng R, Wei C, Tu W, Tang S, Wu F (2011) Simultaneous hyperaccumulation of arsenic and antimony in Cretan brake fern: evidence of plant uptake and subcellular distribution. Microchem J 97:38–43
Feng R, Weic C, Tu S (2013) The roles of selenium in protecting plants against abiotic stresses. Environ Exp Bot 87:58–68
Foyer CH, Noctor G (2005) Oxidant and antioxidant signaling in plants: a reevaluation of the concept of oxidative stress in a physiological context. Plant Cell Environ 28:1066–1071
Fridovich I (1995) Superoxide radical and superoxide dismutases. Annu Rev Biochem 64:97–112
Gill RA, Ali B, Islam F, Farooq MA, Gill MB, Mwamba TM, Zhou WJ (2015) Physiological and molecular analyses of black and yellow seeded *Brassica napus* regulated by 5-aminolivulinic acid under chromium stress. Plant Physiol Biochem 94:130–143
Goupil P, Souguira D, Ferjani E, Faurec O, Hitmid A, Ledoigta G (2009) Expression of stress-related genes in tomato plants exposed to arsenic and chromium in nutrient solution. J Plant Physiol 166:1446–1452
Grispen VMJ, Nelissen HJM, Verkleij JAC (2006) Phytoextraction with *Brassica napus* L.: a tool for sustainable management of heavy metal contaminated soils. Environ Pollut 144:77–83
Gupta M, Sharma P, Sarin NB, Sinha AK (2009) Differential response of arsenic stress in two varieties of *Brassica juncea* L. Chemosphere 74:1201–1208
Gusman GS, Oliveira JA, Farnese FS, Cambraia J (2013) Arsenate and arsenite: the toxic effects on photosynthesis and growth of lettuce plants. Acta Physiol Plant 35:1201–1209
Hoagland D, Arnon D (1941) Physiological aspects of availability of nutrients for plant growth. Soil Sci 51:431–444
Hossain MA, Piyatida P, Jaime A, daSilva T, Fujita M (2012) Molecular mechanism of heavy metal toxicity and tolerance in plants: central role of glutathione in detoxification of reactive oxygen species and methylglyoxal and in heavy metal chelation. J Bot. doi:10.1155/2012/872875
Jain M, Gadre RP (2004) Inhibition of 5-amino levulinic acid dehydratase activity by arsenic in excised etiolated maize leaf segments during greening. J Plant Physiol 161:251–255
Jiang M, Zhang J (2001) Effect of abscisic acid on active oxygen species, antioxidative defence system and oxidative damage in leaves of maize seedlings. Plant Cell Physiol 42:1265–1273
Jiang M, Zhang J (2002) Water stress-induced abscisic acid accumulation triggers the increased generation of reactive oxygen species and up-regulates the activities of antioxidant enzymes in maize leaves. J Exp Bot 53:2401–2410
Leterrier M, Airaki M, Palma JM, Chaki M, Barroso JB, Corpas FJ (2012) Arsenic triggers the nitric oxide (NO) and S-nitrosoglutathione (GSNO) metabolism in Arabidopsis. Environ Pollut 166:136–143
Li WX, Chen TB, Huang ZC, Lei M, Liao XY (2006) Effect of arsenic on chloroplast ultrastructure and calcium distribution in arsenic hyperaccumulator *Pteris vittata* L. Chemosphere 62:803–809
Liao XY, Xie H, Chen TB, Xiao XY, Yan XL, Qu LM, Wu B (2007) Ultrastructure and subcellular distributions of arsenic and calcium in *Pteris vittata* L. Plant Nutr Fertil Sci 13:305–312 **(in Chinese)**
Livak KJ, Schmittgen TD (2001) Analysis of relative gene expression data using real-time quantitative PCR and the $2^{-\Delta\Delta CT}$ method. Methods 25:402–408
Luo H, Li H, Zhang X, Fu J (2011) Antioxidant responses and gene expression in perennial ryegrass (*Lolium perenne* L.) under cadmium stress. Ecotoxicology 20:770–778
Mahdieh S, Ghaderian S, Karimi MN (2013) Effect of arsenic on germination, photosynthesis and growth parameters of two winter wheat varieties in Iran. J Plant Nutr 36:651–664
Megateli S, Semsari S, Couderchet M (2009) Toxicity and removal of heavy metals (cadmium, copper, and zinc) by *Lemna gibba*. Ecotoxicol Environ Safe 72:1774–1780
Meharg AA, Hartley-Whitaker J (2002) Arsenic uptake and metabolism in arsenic resistant and nonresistant plant species. New Phytol 154:29–43
Milioni D, Hatzopoulos P (1997) Genomic organization of hsp90 gene family in Arabidopsis. Plant Mol Biol 35:955–961
Momoh EJJ, Zhou WJ (2001) Growth and yield responses to plant density and stage of transplanting in winter oilseed rape (*Brassica napus* L.). J Agron Crop Sci 186:253–259
Nakano Y, Asada K (1981) Hydrogen-peroxide is scavenged by ascorbate-specific peroxidase in spinach-chloroplasts. Plant Cell Physiol 22:867–880
Panda SK, Matsumoto H (2010) Changes in antioxidant gene expression and induction of oxidative stress in pea (*Pisum sativum* L.) under Al stress. Biometals 23:753–762
Pigna M, Cozzolino V, Violante A, Meharg AA (2009) Influence of phosphate on the arsenic uptake by wheat (*Triticum durum* L.) irrigated with arsenic solutions at three different concentrations. Water Air Soil Pollut 197:371–380
Porra RJ, Thompson WA, Kriedemann PE (1989) Determination of accurate extinction coefficients and simultaneous equations for assaying chlorophylls *a* and *b* extracted with four different solvents: verification of the concentration of chlorophyll standards by atomic absorption spectroscopy. Biochim Biophys Acta 975:384–394
Rahmana MA, Hasegawa H, Rahman MM, Islam MN, Miahc MAM, Tasmen A (2007) Effect of arsenic on photosynthesis, growth and yield of five widely cultivated rice (*Oryza sativa* L.) varieties in Bangladesh. Chemosphere 67:1072–1079
Romero-Puertas MC, Rodriguez-Serrano M, Corpas FJ, Gomez M, del Rio LA, Sandalio LM (2004) Cadmium-induced subcellular accumulation of $O_2^{\bullet-}$ and H_2O_2 in pea leaves. Plant Cell Environ 27:1122–1134
Rout JY, Sahoo RSL (2013) Antioxidant enzyme gene expression in response to copper stress in *Withania somnifera* L. Plant Growth Regul 71:95–99
Schutzendubel A, Polle A (2002) Plant responses to abiotic stresses: heavy metal-induced oxidative stress and protection by mycorrhization. J Exp Bot 53:1351–1365

Seregin IV, Ivanov VB (1997) Histochemical investigation of cadmium and lead distribution in plants. Russ J Plant Physiol 44:791–796

Shanker AK (2008) Mode of action and toxicity of trace elements. In: MNV Prasad (ed) Trace elements as contaminants and nutrients: consequences in ecosystems and human health. Wiley, Hoboken. doi:10.1002/9780470370124.ch21

Sharma I (2012) Arsenic induced oxidative stress in plants. Biolgia 67:447–453

Shen S, Li XF, Cullen WR, Weinfeld M, Le XC (2013) Arsenic binding to proteins. Chem Rev 113:7769–7792

Shri M, Kumar S, Chakrabarty D, Kumar PT, Mallick S, Misra P, Shukla D, Mishra S, Srivastava S, Tripathi RD, Tuli R (2009) Effect of arsenic on growth, oxidative stress, and antioxidant system in rice seedlings. Ecotoxicol Environ Safe 72:1102–1110

Singh N, Ma LQ, Rathinasabapathi BM (2006) Metabolic adaptations to arsenic-induced oxidative stress in *Pteris vittata* L. and *Pteris ensiformis* L. Plant Sci 170:274–282

Srivastava M, Ma LQ, Singh N, Singh S (2006) Antioxidant responses of hyperaccumulator and sensitive Fern species to arsenic. Environ Exp Bot 56:1335–1342

Sun L, Yan XL, Liao XY, Wen Y, Chong ZY, Liang T (2011) Interactions of arsenic and phenanthrene on their uptake and antioxidative response in *Pteris vittata* L. Environ Pollut 159:3398–3405

Thordal-Christensen H, Zhang Z, Wei YD, Collinge DB (1997) Subcellular localization of H_2O_2 in plants. H_2O_2 accumulation in papillae and hypersensitive response during the barley-powdery mildew reaction. Plant J 11:1187–1194

Tombuloglu H, Semizoglu N, Sakcali S, Kekec G (2012) Boron induced expression of some stress-related genes in tomato. Chemosphere 86:433–438

Velikova V, Yordanov I, Edreva A (2000) Oxidative stress and some antioxidant systems in acid rain-treated bean plants. Plant Sci 151:59–66

Verma S, Dubey RS (2003) Led toxicity induces lipid peroxidation and alters the activities of antioxidants enzymes in growing rice plants. Plant Sci 164:645–655

Wang L, Yang L, Yang F, Li X, Song Y, Wang X, Hu X (2010) Involvements of H_2O_2 and metallothionein in NO-mediated tomato tolerance to copper toxicity. J Plant Physiol 167:1298–1306

Wu Z, Mc Grouther K, Chen D, Wu W, Wang H (2013) Subcellular distribution of metals within *Brassica chinensis* L. in response to elevated lead and chromium stress. J Agric Food Chem 61:4715–4722

Xiong J, An LY, Lu H, Zhu C (2009) Exogenous nitric oxide enhances cadmium tolerance of rice by increasing pectin and hemicellulose contents in root cell wall. Planta 230:755–765

Zeng F, Zhou W, Qiu B, Ali S, Wu F, Zhang G (2011) Subcellular distribution and chemical forms of chromium in rice plants suffering from different levels of chromium toxicity. J Plant Nutr Soil Sci 174:249–256

Zhang WF, Zhang F, Raziuddin R, Gong HJ, Yang ZM, Lu L, Ye QF, Zhou WJ (2008) Effects of 5-aminolevulinic acid on oilseed rape seedling growth under herbicide toxicity stress. J Plant Growth Regul 27:159–169

Zhao FJ, Ma JF, Meharg AA, McGrath SP (2009) Arsenic uptake and metabolism in plants. New Phytol 181:777–794

Zhou WJ, Leul M (1999) Uniconazole-induced tolerance of rape plants to heat stress in relation to changes in hormonal levels, enzyme activities and lipid peroxidation. Plant Growth Regul 27:99–104

Zhou YQ, Huang SZ, Yu SL, Gu JG, Zhao JZ, Han YL, Fu JJ (2010) The physiological response and sub-cellular localization of lead and cadmium in *Iris pseudacorus* L. Ecotoxicology 19:69–76